Research on Engineering Structures & Materials
www.jresm.org
MIM Research Group

Research Article

Experimental and numerical investigation of solid and hollow recycled aggregate concrete beams subjected to torsion

Nilesh Masne*[,1,a], Akshay Pawar[2,b]

[1]*Department of Civil Engineering, GES R.H.Sapat College of Engineering Management Studies & Research Nashik (MS), 422005, India*
[2]*Department of Applied Sciences and Humanities, SVKM's College of Engineering, Shirpur (MS), 425405, India*

Article Info

Article History:

Received 20 Sep 2024
Accepted 05 Dec 2024

Keywords:

Abaqus;
Hollow beam;
Recycled aggregate;
Concrete;
Solid Beam;
Torsion

Abstract

To attain sustainable development there is an increasing need of appropriate substitute materials of concrete ingredients such as coarse aggregates. The main aspiration of this effort is to produce the concrete using recycled concrete aggregates derived from construction and demolition (C&D) waste. As such, the use of recycled aggregate concrete (RAC) in structural elements becomes absolutely essential. A series of solid and hollow RAC beams were tested experimentally and simulated under torsional load to compared with natural aggregate concrete (NAC) beams. All tested solid and hollow beams of size, 150 mm wide x 250 mm depth x 1800 mm length with 50 mm x 150 mm opening for hollow beam, which composed of recycled concrete aggregate with replacement ratios of 0%, 50%, and 100%. The torsional capacity of hollow beams was found only lower by 5.49 %, 6.69 % and 8.67 % than the experimental solid beams in test results. The simulation results yielded similar trends, with reductions of 7.52%, 7.90%, and 8.26% in the torsional capacity of hollow beams compared to solid beams. The observed torsional parameter of beams such as crack pattern, torsional ability and twisting angle were found comparable with FE analysis. The findings of this study reveal that RAC beams, whether solid or hollow, possess sufficient torsional capacity and structural integrity, as good as to that of NAC beams. This suggests that RAC can be effectively utilized in structural applications subjected to torsional loads.

1. Introduction

Torsion is the one main structural action in ultimate limit state method and it is the subject of scientific research studies since long time. In 21st century many engineering structures are subjected to torsion because of structural geometry and unbalance loading. Eccentric box girders, curved beams and spiral staircases are some different structures subjected to torsion and the behaviour of these structures dominate due to torsion. Till date, pure torsion is an active research area on traditional reinforced concrete material with recycled concrete aggregate concretes. In accordance with its mix-proportion and cement content, the RAC might have an excellent compressive and tensile strength. There is a compelling need for the civil engineering profession to concentrate on the research, development, and application of innovative materials for modern infrastructure [1-3]. RAC is becoming crucial in structural applications. [4-5]. The RAC attracted a lot of researchers in the last two decades to investigate its performance under different load action such as shear and flexural loading. Fatifazl et al. [6] and Kang et al. [7] found that existing flexural theory applies to reinforced recycled concrete beams, with minimal changes in flexural behavior.

*Corresponding author: nilesh.masne@ges-coengg.org
[a]orcid.org/0000-0003-2146-910X; [b]orcid.org/0000-0003-4902-2182
DOI: http://dx.doi.org/10.17515/resm2024.457me0920rs

A similar tendency was found when recycled concrete compared with conventional concrete in service, yielding and ultimate state results in flexure [8]. The substitution of recycled concrete aggregate in structural concrete has a minor change on the shear parameter [9-10]. Infrequent research work on hollow recycled concrete aggregate concrete beam in torsion has been found in the literature. Some important investigations exist on the failure pattern as well as overall torsional behaviour of hollow beams with NAC and other type of concretes. Hollow concrete sections are gaining popularity in the construction of offshore structures, towers, buildings, and bridges, particularly for accommodating mechanical pipelines and electrical services. The hollow concrete beams reduce structure weight, which affects transport, handling, and erection costs [11]. The hollow beam crack at lower torque than solid beam and ultimate strengths were same for both beams with same strength, size, and reinforcement [12-13]. Torsion causes solid and hollow beams to collapse with 10 % below design loads [14]. Torsional shear stress flows around the section's periphery, peaking at the outside fiber and decreasing away from the surface [15]. The solid and hollow beams responded similarly in shear and torsion [16]. The comparison of experimental results with various code provisions was done and found that the ACI 318-02 code was gave good predictions for the ultimate torsion of hollow beams in pure torsion [17]. The solid and hollow beams of equal size and reinforcement collapse under the equal stress in pure torsion [18–19]. The torsional ductility gets more challenging with increasing concrete strength in hollow beams [20-21]. The hollow RC member cracking torque values are lower than solid member values [22]. The opening size affects the hollow beam capacity under torsion, flexure, and cyclic loading in the EFM analysis [23]. Recent studies have explored the torsional behavior of solid RAC beams, revealing satisfactory torsional performance comparable to NAC solid beams [24-27]. These findings suggest the potential suitability of RAC for structural concrete applications. Untreated coarse recycled concrete aggregate is limited to 40% in concrete grades up to M30, while treated coarse recycled concrete aggregate can be used as a full replacement. This was ascribed to the enhancement in the interfacial transition zone (ITZ) [28]. Self-sensing concrete made from recycled aggregate is more effective at stress-sensing than existing structural health monitoring approaches. This novel material could revolutionize SHM by monitoring structures in real time, improving safety and maintenance [29]. Sustainable construction relies on waste materials in concrete to conserve the environment and improve concrete qualities. To obtain required concrete characteristics and performance, coarse aggregate replacement percentage must be carefully considered [30-33]. The economic feasibility of new civil engineering material as compared to available material is very important in the view of future demand [34]. In order to evaluate whether RAC can be useful for structural use or not, many civil engineers and the researchers has been extensively studied the types of loading tests of solid RAC beams. To the author's knowledge, there is a noticeable lack of experimental and numerical investigations in the existing literature on the structural behavior of hollow RAC beams under torsion. In an effort to address this gap the objective were finalized; the investigation of various properties of recycled aggregate concrete, assess code provisions for torsion, and validate through beam tests and FEA simulation. This study aims to promote the safe and effective use of recycled concrete aggregate in concrete beams.

2. Experimental Materials and Test Setup

2.1. Materials

This investigation utilized OPC 53-grade cement had specific gravity 3.14, fineness 3080 cm^2/g, and 55.5 MPa compressive strength that adhered to the specifications outlined in IS:12269 [35]. Fine Aggregates (FA) of nominal maximum size 4.75mm, fineness modulus = 2.80, water absorption 3.50%, specific gravity 2.65, and Natural Coarse Aggregates (NCA) fineness modulus = 6.70, maximum nominal size 20 mm, specific gravity 2.65, Impact test value 18.18% and crushing value 21.21% meeting the requirements of IS: 383 [36] were used in this study. In compliance with IS: 456 [37], for concreting and curing purposes tap water was used. A chemical admixture meeting the requirements of IS: 9103 [38] was employed to attain the required workability of the concrete. TMT deformed steel bars having average yield strength 515 MPa were used as beam reinforcement and tested as per the practice suggested in IS: 1608 [39]. Concrete cylinders (150 mm x 300 mm) were prepared using steel molds for the purpose of conducting tensile and compressive strength tests.

2.2. Recycled Concrete Aggregates

Rapid urbanization and infrastructural development are consuming natural resources rapidly. Reusing and recycling recycled concrete aggregate was necessary because to rising demand for natural aggregates [40-41]. Construction waste from building and demolition processes must be reduced. In this study, recycled concrete aggregate was sourced from waste concrete panels obtained from demolished reinforced concrete structures [42-43]. Fig.1 showed flow chart of the C&D waste process plant, because the actual photography of plant was not permitted.

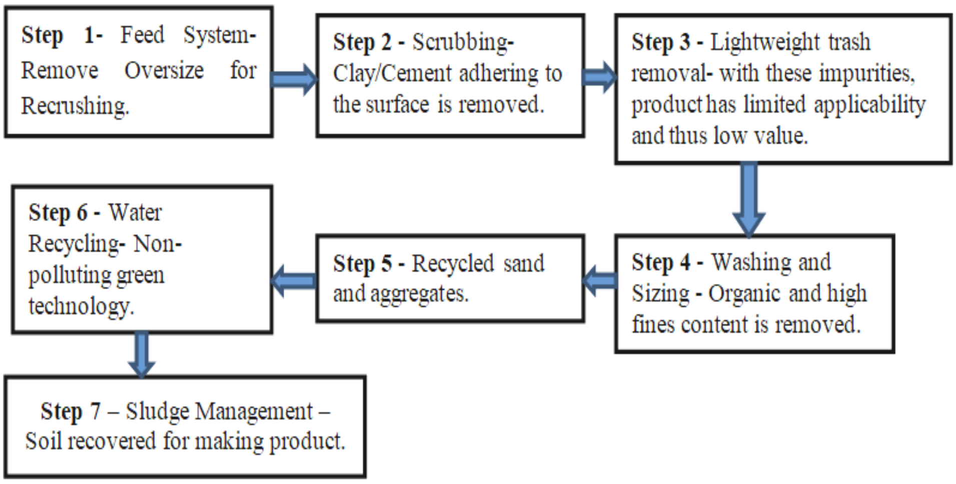

Fig. 1. Flowchart of Processing plant

Fig. 2a showed the concrete panels at the C&D waste center to crush in to required range using a processing plant machine shown in Fig. 2b. After the complete processing on waste concrete lumps, recycled concrete aggregate were transported to working lab for further testing and use shown in Fig.2 (c) and grinding machine shown in Fig. 2 (d) was also used to converts concrete waste into aggregates. The recycled concrete aggregates were categorized into four size fractions (16-20 mm, 12.5-16 mm, 10-12.5 mm, 4.75-10 mm) and stored separately. The recycled coarse aggregate fractions were manually blended to match the grading curve of natural coarse aggregate, conforming to the specifications outlined in IS 383 [36].

Table 1. Coarse Aggregates Properties

Properties	Maximum Size (mm)	Moisture Content (%)	Fineness Modulus	Bulk density (kg/m^3)	Specific gravity	Water absorption (%)	Impact value (%)	Crushing value (%)
Natural Coarse Aggregate	20	0.55	6.66	1530	2.64	0.55	18.58	20.16
Recycled Concrete Aggregate	20	2.31	6.32	1420	2.43	3.59	20.88	22.72

(a)

(b)

(c)

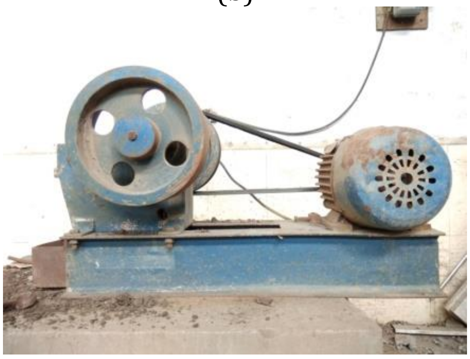

(d)

Fig. 2. (a) Waste concrete panels (b) Crushed concrete lumps (c) Recycled concrete aggregates (d) Grinding machine

2.3. Details of Solid and Hollow Beam Specimens

Three pairs (two each) solid and hollow beams with 0%, 50%, and 100% recycled concrete aggregate beams were cast and tested. The beams measured in length 1800 mm, width 150 mm, and depth 250 mm, with standardized reinforcement, with longitudinal top and bottom reinforcement of 3ø12 and 2ø10 respectively.

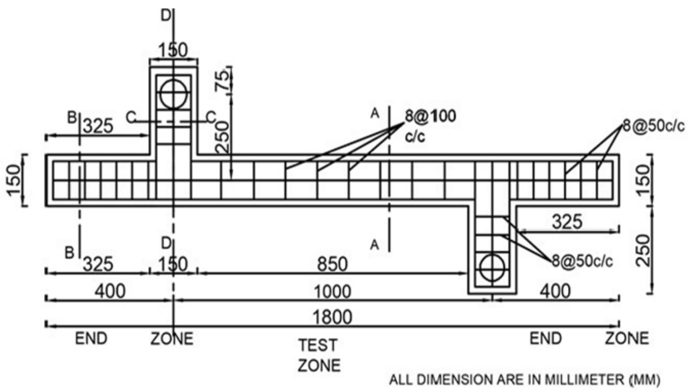

(a)

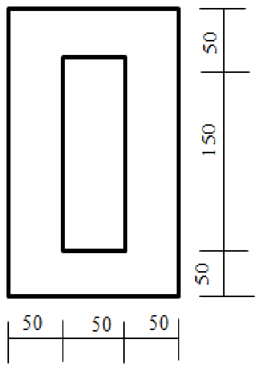

(b)

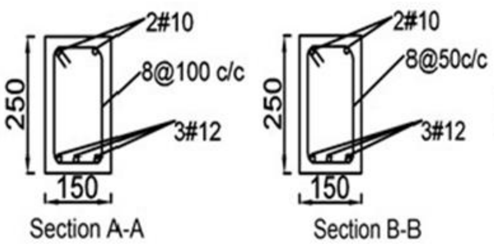

(c)

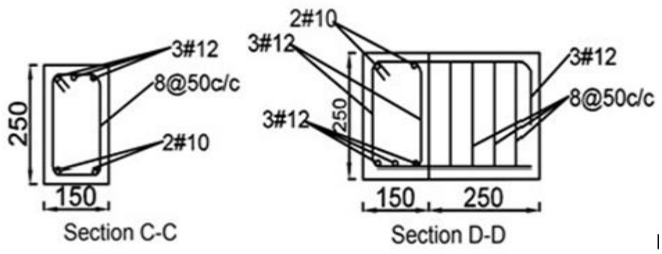

(d)

Fig. 3. Reinforcement Detailing for Solid and Hollow Beams

8mmø @100mm c/c closed stirrups was provided in the test zone. 250 mm x 150 mm Lever arm was provided for applying torque with reinforcement shown in Fig.3 (a). Hollow beams featured a 50mm x 150mm core, surrounded by a 50mm peripheral wall thickness, as illustrated in Fig. 3(b). To cast these beams, 150mm x 250mm end plates with 50mm x 150mm openings were employed. Plywood sheets wrapped with cardboard were inserted to form openings along the beam's length. After 24 hours, the hollow beams were demolded, and the plywood sheets were carefully removed to maintain the wall thickness, which significantly affects the torque and twist values of the hollow beams. The section A-A taken in the test region and section B-B taken in the end zone as shown in the Fig. 3 (c). The section C-C and section D-D taken in the lever arm zone as shown in the Fig.3 (d).

2.4. Concrete Proportioning

A concrete mix design conforming to M30 grade was developed according to IS: 10262 [44], employing the absolute volume method. Recycled concrete aggregate was in the SSD state to maintain constant free water and workability. The volume replacement method was employed, considering the specific gravity difference between natural coarse aggregate and recycled concrete aggregate. Three series of mixtures were prepared as mention in Table 2. The concrete mixtures were named as follows: "M" indicated the mixture, and "R" represented the alternate % of natural coarse aggregate with recycled concrete aggregate.

Table 2. Concrete mix proportion (1 m^3) in Kg

Mix	Cement	Water	Sand	Natural Coarse Aggregate	Recycled Concrete Aggregate
M-R00	380	180	680	1160	000
M-R50	380	180	675	567	552
M-R100	380	180	620	000	1130

2.5. Batching, Mixing and Casting of Concrete Beams

Concrete mixing was performed in the lab in a tilting-drum mixer. Weighed and bagged materials were mixed in a specific sequence. The mixing process involved moistening coarse aggregates with 1/3 of the entire water, followed by addition of 1/3 of the cement. The residual fine aggregates, cement and water, were added, and the mixture was blended thoroughly. The mixed concrete was then transported, poured into molds, compacted, and finished before the initial setting time. The interior surfaces of the molds were coated with shutter oil. For hollow beam casting, 150 x 250 mm end plates with 50 x 150 mm openings and 50 mm peripheral wall thickness were used. Plywood plates wrapped with cardboard were inserted to create openings along the beam's length shown in Fig. 4a. After 24 hours, the plywood plates were carefully removed shown in Fig. 4b, and the cardboard was removed by sprinkling water. The concrete was compacted using a needle vibrator as shown in Fig. 4c. The beam specimens were demolded after 24 hours, then wrapped in gunny bags and cured on a clean, level laboratory floor.

(a)

(b)

(c)

Fig. 4. Casting of beams

2.6. Instrumentation and Test Setup

A custom setup for test was planned to apply torsion to the beam specimen. As revealed in Fig. 5, the beam was placed on roller supports, allowing its ends to rotate, extend, and contract freely. The strategic placement of roller supports at both ends prevented longitudinal compression, ensuring that the beam was subjected to torsion only.

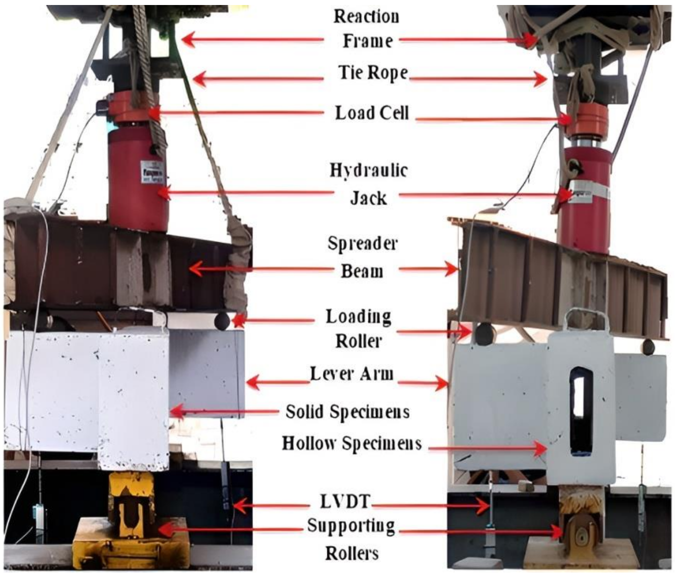

Fig. 5. Solid and hollow beam torsion test setup

Torsion was applied to a 850 mm free span, within an effective range of 1000mm. Vertical deformations were recorded by two LVDTs positioned beneath the soffit of two lever arms. The load sensor and LVDT were connected to a data acquisition system. All the beams were subjected to progressive loading at its center, using a 1000kN hydraulic jack, with incremental load increments until failure.

3. Results and Discussion

3.1Fresh Concrete Slump

The inferior slump values of RAC mixes, compared to NAC mixes, can be attributed to the irregular shape and lower specific gravity of recycled concrete aggregate relative to natural coarse aggregate. The recycled concrete aggregate has an older recycled concrete aggregate-cement bond that is different from the new cement bond. This makes it harder for RAC to flow. To get the right slump for RAC, super plasticizer must be used in RAC, just like it is needed for recycled concrete aggregate, which has an odd shape. So, adding super plasticizer to RAC made it similar to NAC in that it was easy to work with and compacted well. Consequently, the addition of super plasticizer to RAC allowed RAC to attain comparable workability and compaction to that of NAC. All mixes were planned to slump in the S3 slump class (100-150 mm).

3.2 Density of Concrete

The density of RAC decreased linearly with increasing replacement ratios of natural coarse aggregate to recycled concrete aggregate, yielding lower densities compared to NAC. Table 3 shows that RAC mixes containing 50% and 100% RCA had densities 1.92% and 3.75% lower, respectively, than NAC. This trend is attributed to the direct relationship between concrete density and the density of its constituent particles.

3.3. Mechanical Properties of Concrete

To evaluate the compressive and tensile strength of each mix, cylinders of 150 mm x 300 mm were made according to IS: 516 [45] and IS: 5816 [46]. The beams were given the following names in Table 3: (1) the solid and hollow beams marked by SB and HB. (2) R shows the % of replacement of recycled concrete aggregate.

Table 3. Measured properties of concrete

Beam Id	Density (Kg/m^3)	Compressive Strength (MPa)	Tensile Strength (MPa)
SB-R00	2400	37.55	4.11
HB-R00	2400	37.45	4.11
SB-R50	2354	36.85	3.98
HB-R50	2354	36.82	3.97
SB-R100	2310	32.33	3.15
HB-R100	2310	32.36	3.11

The types of failure did not show any significant variations. The NAC and RAC had approximately equal ultimate compressive strength for each pair of beams as shown in Table 3. The 50% and 100 % recycled concrete aggregate mixes were lower than natural coarse aggregate i.e.1.6 % and 5.1 % respectively. The equivalent strength of concrete mixes may be justified by the particle shape, their adherence to the paste of cement and caliber of concrete. Compared to natural coarse aggregate concrete, the tensile strength reductions of 3.41% and 14.63% were observed for 50% and 100% recycled concrete aggregate concrete, respectively. The strong attachment between the cement paste and recycled aggregate, facilitated by the aggregate's rough and porous texture, may contribute to this reduction. The tensile strength was influenced more by the recycled concrete aggregate's quality rather of their amount [47]. It is abundantly evident that if the recycled aggregates are employed in the SSD state, replacing natural aggregates by recycled aggregates at whatever percentage leads only in a minor difference in concrete slump. The concrete mix achieved the desired compressive strength (30 MPa) at 28-day. Although moisture conditions of the coarse aggregates affected compressive strength, replacing natural aggregate with recycled aggregate proved beneficial. Importantly, this substitution did not significantly impact the concrete's workability, compressive strength, or tensile strength.

3.4. Effect of Recycled Concrete Aggregate on Cracking Behaviour of Solid and Hollow Beams

This analysis included the examination of propagation with failure patterns of cracks. The test revealed that the tensile cracking about all faces of the RAC and NAC beams. There were no visible fractures in any of the beams as the torque was progressively increased at the start of the test. Fig. 6 illustrates the cracking and failure patterns of RAC beams with varying replacement ratios. The results indicate a positive correlation between the replacement ratio and the number of cracks, with an increase in cracks as the replacement ratio increased. Diagonal cracks appeared on both wider and shorter faces, simultaneously. As torque increased, cracks on the larger faces shifted towards the shorter faces, at right angles to the longitudinal beam's axis. Identified cracks joined with original 45-degree cracks on shorter faces, resulting in S-shaped curves. The results show that recycled concrete aggregate in solid and hollow beams promotes numerous cracks and stress redeployment subsequent to original cracking. Key findings include are (1) RAC beams developed multiple diagonal cracks after the first crack. (2) Cracks and twist angles increased with torque. (3) A notable diagonal break occurred at 45-48 degrees from the beam axis. (4)RCA increased the diagonal crack angle in solid and hollow beams. (5) The test results showed that hollow beams exhibited cracking and failure at marginally lower loads compared to solid beams. This suggests that the concrete core in solid beams plays a beneficial role in enhancing the cracking load.

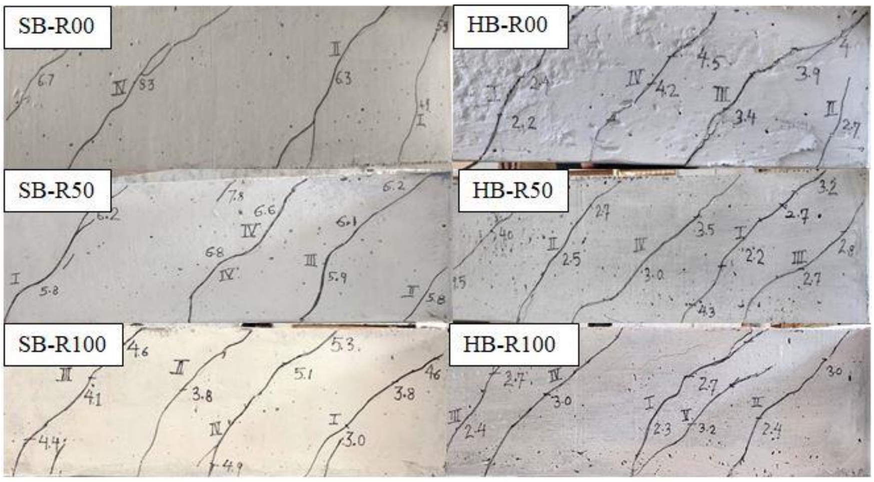

Fig. 6. Cracks pattern in test region of solid and hollow beams

3.5. Effect of Recycled Concrete Aggregate on Torque and Twist angle

The hollow RAC beams exhibited lower cracking resistance and maximum rotational force compared to solid NAC beams, which showed minimal damage. Table 4 indicates that as the proportion of recycled concrete aggregate in the beam increased, the torsional strength decreased, while the angle of twist increased.

Table 4. Measured torque and twist angle

Beam ID	Cracking State		Ultimate State	
	T_{cr} (kN.m)	θ_{cr} (rad/m)	T_u (kN.m)	θ_u (rad/m)
SB-R00	3.68	0.003	11.10	0.027
HB-R00	3.11	0.003	10.51	0.028
SB-R50	3.40	0.003	10.44	0.027
HB-R50	2.87	0.003	9.76	0.029
SB-R100	2.89	0.004	9.82	0.031
HB-R100	2.71	0.006	8.97	0.033

The torsional capacity of the beams was only reduced by 5.49% and angle of twist was increases by 3.70% for HB-R00. The torsional capacity of the beams was only reduced by 6.69% and angle of twist was increases by 6.89 % for HB-R50. The torsional capacity of the beams was only reduced by 8.67% and angle of twist was increases by 9.09% for HB-R100 at ultimate state as compared to that of SB-R00, SB-R50 and SB-R100 beams. Both beams had about the equivalent force resistance capacity, but solid beams had a little more. The strength of hollow beams was identical to that found in the solid beams. The concrete core's absence was the lone deviation. Both series points lie on the same curve, indicating that similar reinforcing levels resulted in nearly equal torsion ultimate strengths. The results suggest that the concrete core does not provide a significant contribution to the ultimate torsional strength of a solid beam, and the torque was not caused by the concrete core's resistance as is generally believed. It will help figure out what changes need to be made to the current standards and how to use RAC solid and hollow beams for building structures. The lesser modulus of elasticity of RAC compare to NAC results in increased twist angles, especially with higher recycled concrete aggregate ratios under different stress conditions. Nevertheless, hollow RAC beams exhibit acceptable behavior, albeit slightly inferior, compared to solid RAC beams at all loading stages in torsion.

3.6. Effect of Recycled Concrete Aggregate on Torque-Twist Relationship

It can be understood from Fig.7 the hollow beams perform nearly well with solid beams in test results. The fact that both series points are on the same curve suggests that equivalent torsion ultimate strengths were produced by comparable levels of reinforcing. As a result, it appears that the concrete core did not increase a solid beam's final torsional strength, and contrary to popular belief, the torque was not brought on by the resistance of the concrete core.

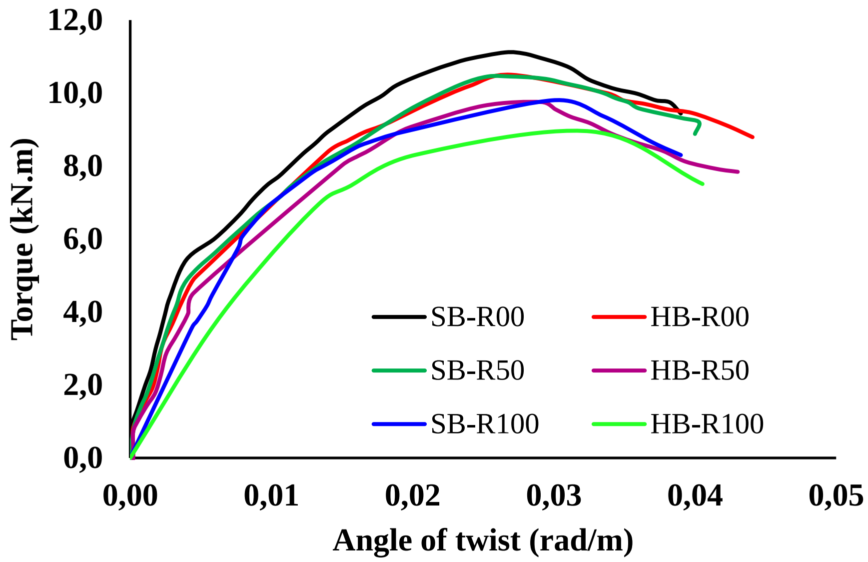

Fig. 7. Measured Torque-Twist curves for all tested beams

For the solid beam, the peak torsional moment was 11.10kN.m, for the hollow beam it was 10.51kN.m, and for the solid beam it was 9.76kN.m. The peak torsional moment for the solid beam was 10.44kN.m. The measured twist angles for solid and hollow beams were 0.027rad/m, 0.027rad/m, 0.031 rad/m and 0.028rad/m, 0.029rad/m, 0.033rad/m, respectively for 0%, 50%, and 100% replacement of recycled concrete aggregate. The final torque and angle of twist was not affected to a great extent because of the replacement ratio of recycled concrete aggregate. However, the consequence was not big adequate to stop using recycled concrete aggregate in RAC beams for pure torsion in solid and hollow beams. Form the achieved results, the torsional behaviour, angle of twist and crack pattern at every state loading with the failure mode of varying % of RAC in solid and hollow beams it can be committed that the application of RAC in structural use under torsion is feasible with prior care.

4. Validation of Laboratory Tested Beams by Finite Element Method

The increasing use of finite element analysis to simulate the complicated structural issues ABAQUS, ATENA-3D, ANSYS, LS-Dyna and some other software are available. These FE software's help to analyses the structural concrete element under the variety of loading such as flexure, shear and torsion. The accuracy of FE model based on compatibility of non-linear method and adopted materials model. This study simulated hollow and solid beams with coarse RCA subjected to torsion using ABAQUS FEA software. The simple object method was used to create geometry in ABAQUS. The brittle-cracking model was adapted as a material model, which yield better results of concrete. Simple Rankine yield criterion was employed to perceive accurate crack initiations and propagations on the beams, which allows the crack closing and reopening. The top of the beam was loaded via displacement-controlled method to match the spreader beam center deformation rate. The rigid steel roller support was vertically constrained and modeled by a line of contact boundary condition. Monitoring stations were set at the spreader beam top and lever arm soffit to record load and deformation.

4.1. Geometrical Definition and Meshing

A three-dimensional geometrical model of the beam specimens shown in Fig.(a) was developed in ABAQUS utilizing the built-in modeling tools and element library. The Fig. 8 (b) shown longitudinal and transverse directions reinforcement, modeled as truss elements (T3D2) based on experimental details. The reinforcement consisted of 12 mm diameter for bottom steel, 10 mm diameter bars for top reinforcement and 8 mm diameter bars for web reinforcement. Web reinforcement was spaced 100 mm apart to achieve the desired torsion response. ABAQUS effectively modeled curved parts, such as steel rollers, using precise contact shown in Figs. 8 (a) and 8(c). The model employed 25 mm; eight-noded, hexahedral (brick) elements with incompatible modes (C3D8I) to prevent overly rigid behavior under bending. The steel rebars were replicated using 10 mm-sized 3D linear truss (T3D2) elements.

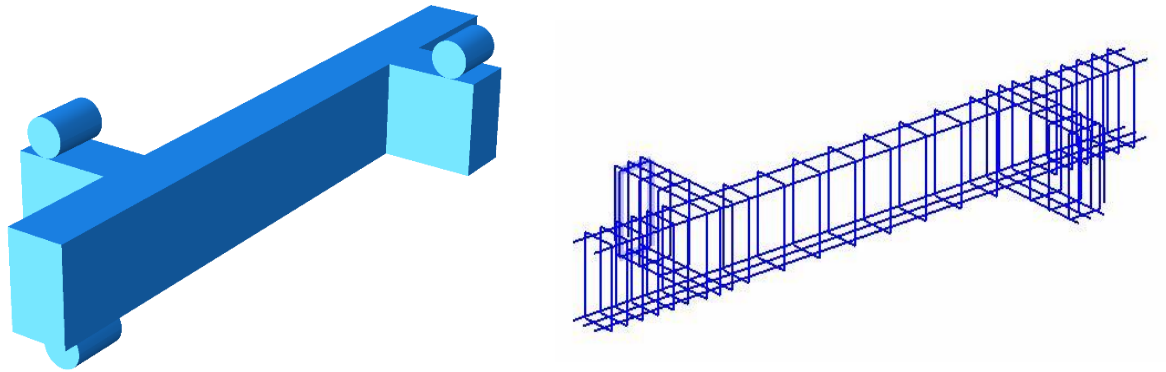

(a) (b)

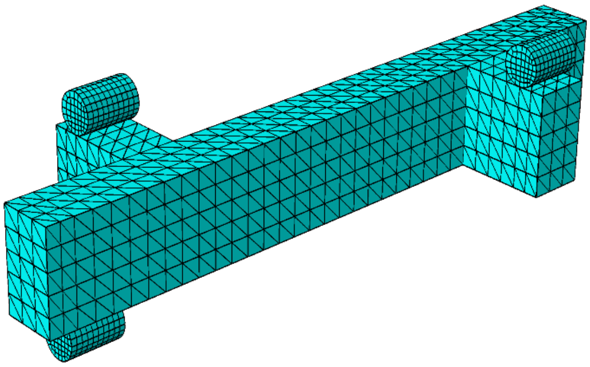

(c)

Fig. 8. Geometrical modelling and meshed beams

4.2. Material Models

For various materials and applications, ABAQUS provides a range of material models. ABAQUS also allows users to create custom material models, a valuable feature when working with unconventional materials. While predefined models suffice for standard concrete structures, they cannot accurately simulate concretes containing alternative ingredients like silica fume, fly ash, or recycled aggregates. To address this limitation, the constitutive model published by Suryawanshi et al. [48] was employed to capture the non-linear performance of NAC and RAC. The simple stress-strain relationship is defined by Eq. 1.

$$\bar{\sigma} = a(\bar{\varepsilon}) + b(\bar{\varepsilon})^2 + c(\bar{\varepsilon})^3 + d(\bar{\varepsilon})^4 \tag{1}$$

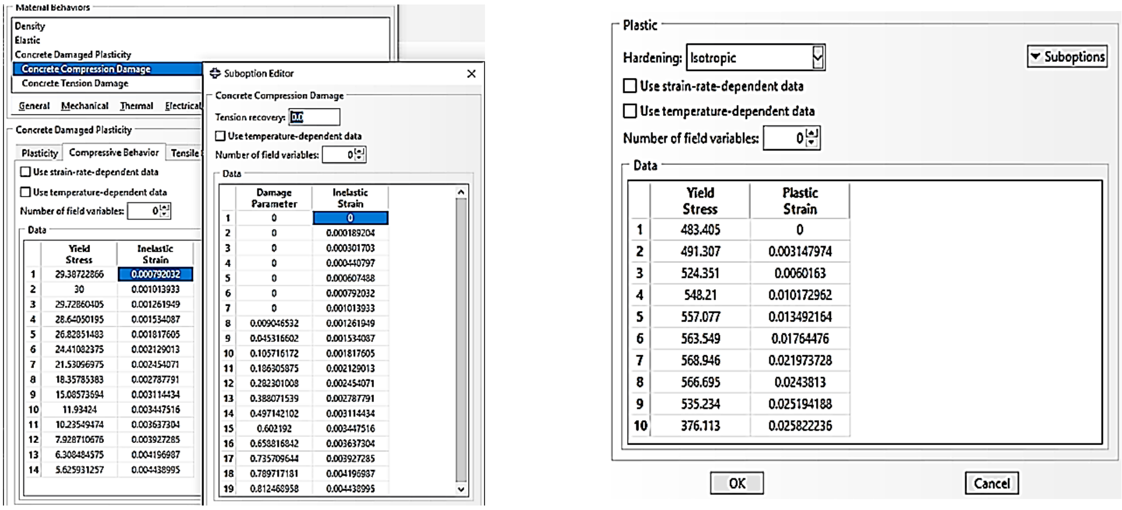

(a) (b)

Fig.9. Input parameter - Stress-strain relations for concrete and reinforcement

Figure 9 (a) shows the window for user-defined material definition using stress-strain data of compression test and inelastic strain damage factors. The Concrete Damage Plasticity model can be characterized using tensile test stress-strain data in conjunction with the associated material damage parameters. According to Earij et al. [49], ABAQUS has adopted appropriate values for input parameters like dilation angle, eccentricity, and viscosity parameters from existing literature. Concrete's compressive and tensile behaviors, as well as its elastic and plastic qualities, are examples of additional material input characteristics. Concrete's non-linear stress-strain behavior must be taken into account when predicting material damage using the damage coefficient. ABAQUS also permits users to incorporate the actual nonlinear stress-strain behavior of steel, thereby enabling more precise simulations compared to idealize elastic-plastic models. The dialogue window appears in Fig.9 (b) after entering stress-strain values. Note that ABAQUS only accepts inelastic strain and stress values. Differentiating total strain and elastic strain yields inelastic strain.

4.3. Cracking Behaviour of Solid and Hollow RAC Beams

In ABAQUS, the bands of principal tensile strain generated during the loading. Tensile strain bands with precise color to represents definite magnitude of strain that can compare with actual crack pattern observed during test. During loading, the crack pattern (principal tensile strain band) was monitored in both beams. The first diagonal crack appeared at the same depth as observed experimentally. As the load increased, the diagonal crack pattern propagated to other faces of the beams, with additional crack bands forming. Figs. 9 and 10 shows that the crack patterns, characterized by principal tensile strain, were comparable in both solid and hollow beams, regardless of the recycled concrete aggregate content.

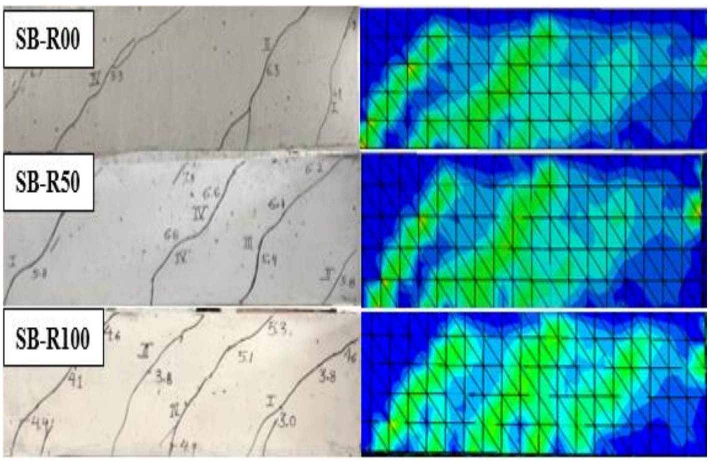

Fig. 9. Comparative crack pattern of solid beams

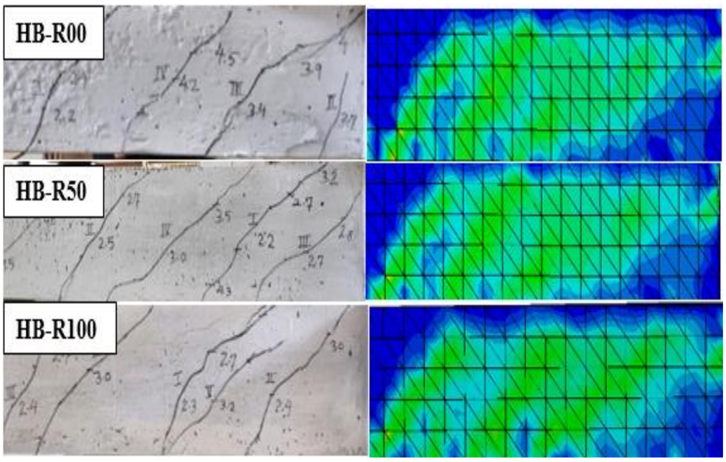

Fig. 10. Comparative crack pattern of Hollow beams

The development of tensile strain bands, characterized by distinct colors indicating particular strain magnitudes, can be correlated with the actual crack patterns found in experimental settings. Figure 9 and 10 illustrates the relationship of fracture pattern in beams with varying substitution amounts of recycled concrete aggregate, alongside the primary tensile strain patterns simulated by ABAQUS. Notably, the major tensile strains patterns produced by ABAQUS and experimental were align with each other. Fig. 10 displays the identical cracking patterns produced by ABAQUS analysis along with cracking patterns that were obtained from experiment. The cracking pattern in all solid and hollow beams with varying percentages of recycled concrete aggregate was identical. All solid beam specimens shown the first crack was almost at somewhat higher torsion than the hollow beam. However, as the percentage of recycled aggregates replacing natural aggregates rise, the peak load falls in both results for all beams. This suggests that RAC-beam and NAC-beam behave similarly in both the tests. The beam containing recycled concrete aggregate 50% and 100% found more cracks than NAC beam in both the test. Hollow beams showed wider crack than the solid beam in experiment test and FEM analysis.

4.4. Torque-Twist Capacity RAC Beams at Ultimate State

All the solid and hollow beam were tested in load frame experimentally and the tested beam validated through finite element software ABAQUS. The load and deformation data were recorded continuously and transform into Torque-Twist form for more analysis. The twisting angle along with torsional ability of all the beams at ultimate state was compared with ABAQUS analysis. Table 5 shows torsional capacity of solid beams somewhat more than hollow beam in both studies. As the % of RCA increase torsional capacity decreases in both the methods.

Table 5. Observed and simulated torsional moment of RAC beam

Beam Id	Ultimate Torsional Moment Measured (kN.m)	Ultimate Torsional Moment ABAQUS (kN.m)	Angle of twist Measured (rad/m)	Angle of twist ABAQUS (rad/m)
SB-R00	11.10	11.70	0.027	0.028
HB-R00	10.51	10.82	0.028	0.031
SB-R50	10.44	10.75	0.027	0.030
HB-R50	9.76	9.90	0.029	0.033
SB-R100	9.82	9.92	0.031	0.032
HB-R100	8.97	9.10	0.033	0.035

The ultimate torsional capacity of experimentally tested solid beams SB-R00, SB-R50 and SB-R100 was decreased by 5.12%, 2.88% and 1% than the numerical torsional value. The ultimate torsional capacity of experimentally tested hollow beam HB-R00, HB-R50 and HB-R100 was decreased by

2.86%, 1.14% and 1% than the numerical torsional value. The torsional ability of hollow beams was found lower by 7.52 %, 7.90 % and 8.26 % than the solid beams in simulation results. From the test results in the both method it was seen that the torsional capacity of ABAQUS software was found nearly close to experimental values at the definitive state for all the beams.

4.5. Torque-Twist Behaviour of RAC Beams

The experimental and numerical results showed similar behavior for hollow and solid beams before and after the peak. However, the ABAQUS simulation yielded a slightly larger area under the torque-twist curve compared to the experimental curve, as illustrated in Fig. 11. The ABAQUS investigation shows a comparable trend of reduced resistance capability of torque and increasing twisting angle at higher replacement levels. This could be due to a decrease concrete modulus of elasticity, which corresponds to a greater extent of natural coarse aggregate substitution.

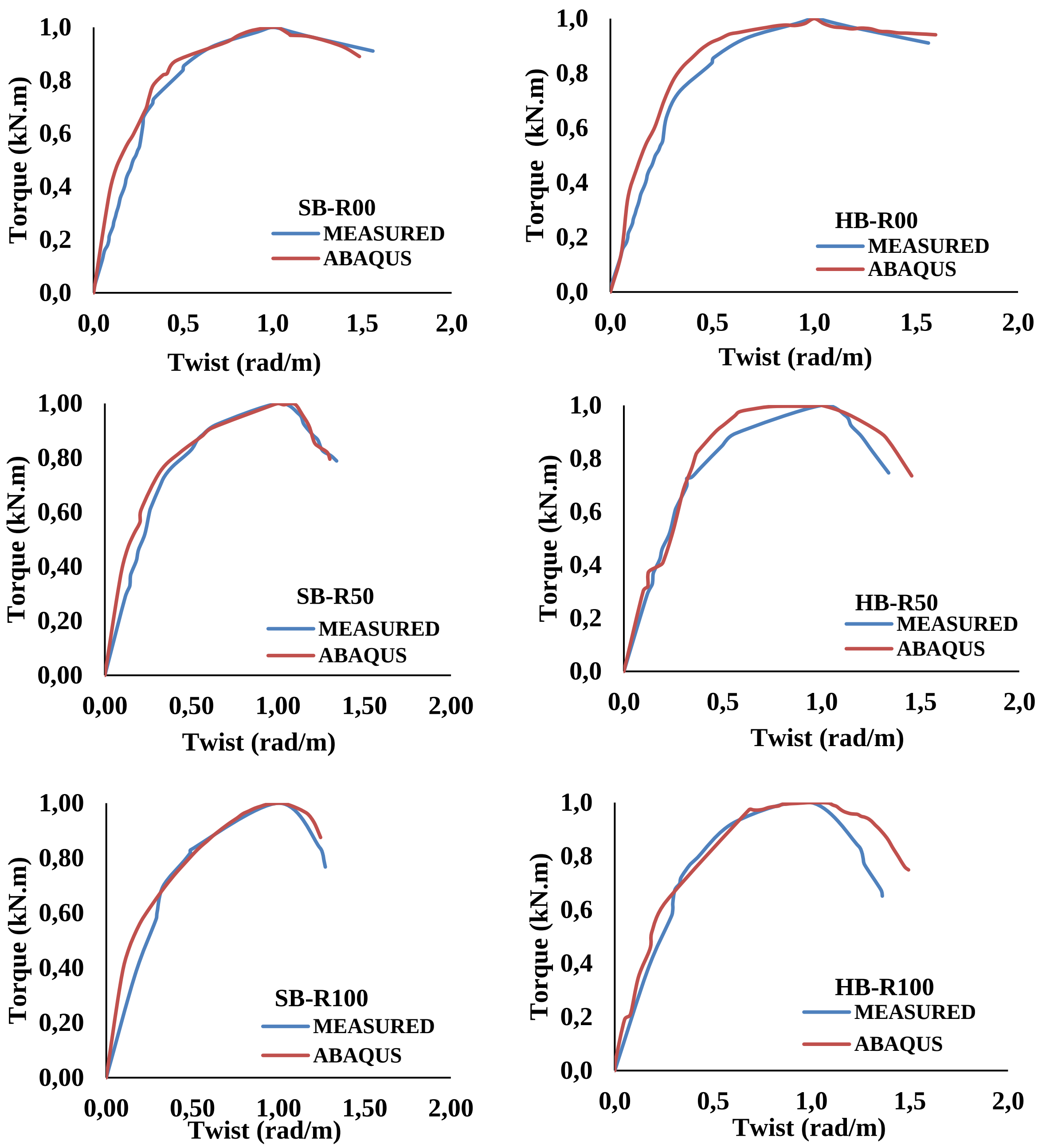

Fig. 11. Comparative torque-twist performance of solid and hollow beam

Fig. 11 displays the torque-twist relationships established by ABAQUS software. The specimens responded virtually linearly after cracking until the tension bar yielded. Following this, each specimen showed nonlinear behavior until reaching its failure load. Enough rotation of the plastic hinge causes high stress in the specimens' compression zone, leading to crushing failure. The experimental torque-twist curves for all solid and hollow beam specimens compared in Fig. 11. Both analyses showed similar torque-twist tendencies. The presence of two interfacial transition zones (ITZs) in RAC beams reduced their cracking stress and stiffness compared to natural NAC beams, which have only one ITZ. This is attributed to the lower modulus of elasticity of RAC.

The torque-twist behavior of solid beam showed somewhat higher torque at cracking state and same at the ultimate state than hollow beams. The experimentally tested 50% and 100% recycled concrete aggregate hollow beam showed lower torque-twist behavior with the comparison of simulation during ultimate to failure state as shown in Fig.11 (HB-R50 and HB-R100). Increasing the replacement level of recycled concrete aggregate reduces the area under the torque-twist curve. Furthermore, the incorporation of recycled concrete aggregate in concrete leads to a more gradual post-peak decline in the torque-twist curves, highlighting the increased weakness of RAC compared to NAC.

5. Conclusions

A numerical investigation was conducted to examine the impact of recycled concrete aggregate on the torsional behavior of reinforced concrete beams, with validation provided by experimental results. The primary findings are outlined below:

- To achieve satisfactory workability, the addition of super plasticizer was found suitable and the concrete density of RAC beam was not affected considerably as compare to NAC.
- The tensile and compressive strength with 0% and 50% recycled concrete aggregate of concrete were found decrease by 3.16% and 1.86% respectively. However, the RAC with 100% recycled concrete aggregate of tensile and compressive strength w.r.t. NAC found decrease by 23.35% and 13.82%. Because of the breakdown of the aggregate-cement paste bond inferior results of RAC was found as compare to NAC.
- Both experimental and numerical results showed similar crack initiation and propagation patterns in solid and hollow beams. Upon reaching maximum torsion, a dominant crack in the test zone expanded significantly, leading to tensile failure of the beams in both experimental and numerical methods.
- Similar diagonal cracks were observed in hollow and solid beam and the beam containing recycled concrete aggregate found more cracks than NAC beam in both the test. Hollow beams showed wider crack than the solid beam in test and FEM analysis.
- The experimental torque of the all hollow beams was found decreased than solid beam by 5.31%, 6.51% and 8.05% at ultimate state with the increased twisting angle and % of recycled concrete aggregate in comparison to solid beams. The twist angle of the beam was increased for HB-R00 by 3.70%, for HB-R50 by 6.89% and for HB-R100 by 9.09% at ultimate state as compare with SB-R00, SB-R50 and SB-R100 beams.
- Increasing the proportion of recycled concrete aggregate (RCA) reduces the area under the torque-twist curve. Moreover, RCA inclusion leads to a more pronounced reduction in the post-peak gradient of the torque-twist curve, indicating increased brittleness in RAC compared to NAC.
- The inclusion of recycled concrete aggregate in structural concrete leads to a reduce in the area under the torque-twist curve as the replacement level increases. Furthermore, the utilize of recycled concrete aggregate reduces the post-peak gradients of the torque-twist curve, highlighting the increased brittleness of RAC compare to NAC.
- The ultimate torsional capacity of experimentally tested solid beams SB-R00, SB-R50 and SB-R100 was decreased by 5.12%, 2.88% and 1% than the numerical torque. The ultimate

torsional capacity of experimentally tested hollow beam HB-R00, HB-R50 and HB-R100 was decreased by 2.86%, 1.14% and 1% than the numerical torque. The torque-twist characteristic revealed that, ABAQUS simulation results were significantly closer to experimental results at all the parameters. This indicates that the significance of sound characterize material definition in expressions of calculated stress-strain relation of yield of numerical simulation.

- The torque-twist behaviour of solid beam showed somewhat higher torque at cracking state and same at the ultimate state than hollow beams. The experimentally tested 50% and 100% recycled concrete aggregate hollow beam showed lower torque-twist behaviour with the comparison of simulation during ultimate to failure state.

According to the findings, additional research is necessary in order to reach an agreement regarding its torsional performance of RAC beams.

References

[1] Patare SA, Bhirud YL. Effect of displacement control gain on the shape of functionally graded piezoelectric beam using a simple beam theory. Asian J Civ. Eng. 2022; 23:887–905. https://doi.org/10.1007/s42107-022-00463-7

[2] Nataraja MC, Bhat G, Manoj M, Mallya S. Investigation on concrete with crushed vitrified tiles as coarse aggregates. J Build Path and Rehabil. 2022;7: 103 https://doi.org/10.1007/s41024-022-00245-3

[3] Manthene SL, Boddepalli KR. Effect of tile aggregate and flyash on durability and mechanical properties of self-compacting concrete. J Build Rehab. 2022; 7, 68 https://doi.org/10.1007/s41024-022-00209-7

[4] Pawar AJ, Suryawanshi SR. Comprehensive Analysis of Stress-strain Relationships for Recycled Aggregate Concrete. Inter J Eng, Transactions B: Applications. 2022; 35(11): 1184-1191. http://dx.doi.org/10.5829/ije.2022.35.11b.05

[5] Masne N, Suryawanshi S. Effect of replacement ratio on the torsional behaviour of recycled aggregate concrete beams. Inter J Eng, Transactions A: Basics. 2023; 36 (04): 659-668. https://doi.org/10.5829/ije.2023.36.04a.06

[6] Fathifazl G, Razaqpur AG, Isgor OB, Abbas A, Fournier B, Foo S. Flexural performance of steel-reinforced recycled concrete beams. ACI St J. 2009; 106 (6): 858-867. https://doi.org/10.14359/51663187

[7] Kang THK, Kim W, Kwak YK, Hong SG. Flexural testing of reinforced concrete beams with recycled concrete aggregates. ACI St J. 2014; 111 (3):607-616. https://doi.org/10.14359/51686622

[8] Seara-Paza S, González-Fonteboab B, Martínez-Abellab F, Eiras-Lópezb J. Flexural performance of reinforced concrete beams made with recycled concrete coarse aggregate. Eng St. 2018; 156:32–45. https://doi.org/10.1016/j.engstruct.2017.11.015

[9] Rahal KN, Alrefaei YT. Shear strength of recycled aggregate concrete beams containing stirrups. Cons and Build Mat. 2018; 191:866–876. https://doi.org/10.1016/j.conbuildmat.2018.10.023

[10] Albostami AS, Al-Hamd Rwayda KS, Alzabeebee S. Shear strength assessment of reinforced recycled aggregate concrete beams without stirrups using soft computing techniques. J Build Path Rehabili.2018;8:98 https://doi.org/10.1007/s41024-023-00343-w

[11] Alshimmeri AJH, Al-Maliki HNG. Structural Behaviour of Reinforced Concrete Hollow Beams under Partial Uniformly Distributed Load. J Eng. 2014; 20 (7): 130-145.

[12] Hsu TTC. Torsion of structural concrete behaviour of reinforced concrete rectangular members torsion of structural concrete pure torsion-reinforced sections. ACI, 1968; Paper SP 18-10, Detroid, 261-306.

[13] Lampert P, Thurlimann BT. Ultimate Strength and Design of Reinforced Concrete Beams in Torsion and Bending. Intern Asso for Bridge and Structural Eng. 1971; 31(1):107-131.

[14] Bhatt P, Ebireri JO. Direct design of beams for combined bending and torsion. Stavebnicky Casopis, Building J (Bratislava). 1989; 37 (4):249–263.

[15] Collins MP, Mitchell D. Pre-stressed concrete structures. Prentice Hall Inc.1991, Englewood Cliffs, NJ.

[16] Fouad E, Ghoneim M, Issa M, Shaheen H. Combined shear and torsion in normal and high strength concrete beams Experimental Study. J Eng App Sci. 2000; 47(6): 1059–1078.

[17] Bernardo L, Lopes S, Oliveira L. Torsion in reinforced high-strength concrete hollow beams. INCOS, 2003; 5:277-286.

[18] Bernardo LFA, Lopes SMR. Behaviour of concrete beams under torsion: NSC plain and hollow beams. Mat and St. 2008; 41:1143–1167. http://dx.doi.org/10.1617/s11527-007-9315

[19] Alnuaimi AS, Al-Jabri KS,Hago A. Comparison between solid and hollow reinforced concrete beams. Mat and St. 2008; 41:269-281. http://dx.doi.org/10.1617/s11527-007-9237-x

[20] Lopes SMR, Bernardo LFA. Cracking and failure mode in HSC hollow beams under torsion. Cons and Buil Mat. 2014; 51: 163–178. http://dx.doi.org/10.1016/j.conbuildmat.2013.10.062

[21] Lopes SMR, Bernardo LFA. Twist behaviour of high-strength concrete hollow beams _Formation of plastic hinges along the length. Eng St. 2009; 31: 138-149. http://dx.doi.org/10.1016/j.engstruct.2008.08.003
[22] Jeng CH, Chao M, Peng SF. Constitutive relationships of concrete for hollow RC members in pure torsion. Mag Con Res. 2014; 66 (17):896–912.
[23] Jabbar S, Hejazi F, Mahmod HM. Effect of an Opening on Reinforced Concrete Hollow Beam Web Under Torsional, Flexural, and Cyclic Loadings. Lat Amer J Sol and St. 2016; 13:1576-1595. https://doi.org/10.1590/1679-782512629
[24] Fu JL, Liu BK, Ma JW, Zhou H. Experimental study on seismic behaviour of recycled aggregate concrete torsion beams with Abaqus Ad Mat Res. 2015; 1079-1080: 220-225. https://doi.org/10.4028/www.scientific.net/AMR.1079-1080.220
[25] Wang X, Liu B, Zhang C. Seismic behaviour of recycled aggregate concrete beams under cyclic torsion. Con and Build Mat. 2016; 129:193–203. http://dx.doi.org/10.1016/j.conbuildmat.2016.10.101
[26] Sarsam KF, Salih N, Hussein M. Assessment of reinforced recycling aggregate concrete beams under torsional moment. Intl J Eng & Tech. 2016; 7 (4.20): 623-628. http://dx.doi.org/10.14419/ijet.v7i4.20.27403
[27] Masne N, Suryawanshi S. Numerical and Experimental Investigation of Recycled Aggregate Concrete Beams Subjected to Pure Torsion. Int J Eng Transactions A: Basics. 2022; 35 (10): 1123-1132. http://dx.doi.org/10.5829/ije.2022.35.10a.14
[28] Ojha PN, Kaura P, Singh B. Studies on mechanical performance of treated and non-treated coarse recycled concrete aggregate and its performance in concrete-an Indian case study. Res. Eng. Struct. Mater. 2024; 10(1): 341-362. : http://dx.doi.org/10.17515/resm2023.53me0728rs
[29] Kumar CA, Reddy PN, Kulkarni AP. Self-sensing concrete with recycled coarse aggregates and multi-walled carbon nanotubes: A sustainable and effective method. Res. Eng. Struct. Mater. 2024; 10(1): 41-56. http://dx.doi.org/10.17515/resm2023.773ma0520
[30] Belmouhoub A, Abdelouahed A, Noui A. Experimental and factorial design of the mechanical and physical properties of concrete containing waste rubber powder. Res. Eng. Struct. Mater. 2024; 10(2): 461-480. http://dx.doi.org/10.17515/resm2023.54me0810rs
[31] Poonam, Singh VP. Response surface methodology use in optimization of concrete properties using blast furnace slag aggregate and recycled concrete sand. Res. Eng. Struct. Mater. 2024; 10(1): 111-133.DOI: http://dx.doi.org/10.17515/resm2023.788me0614
[32] Masne N, Suryawanshi S. Effect of waste water curing and elevated temperature on recycled concrete aggregates from construction and demolition waste. Iranian (Iranica) Journal of Energy & Environment – Peer review Journal. 2023; 4(2): 152-158. https://doi.org/10.5829/IJEE.2023.14.02.07
[33] Masne N, Suryawanshi S. An Investigation of the Mechanical Properties of Recycled Aggregate Concrete with Silica Fume. Sustainable Building Materials and Construction, Lecture Notes in Civil Engineering, Springer, 2022; 222: 379-387. https://doi.org/10.1007/978-981-16-8496-8_47
[34] Hussein Talab Nhabih, Mohammad R. K. M. Al-Badkubi, A. A. El-barbary, Marwa Marza Salman. Recycling harmful plastic waste to produce a fiber equivalent to carbon fiber reinforced polymer for reinforcement and rehabilitation of structural members. Curved and Layered Structures. 2024; 11: 20240003. https://doi.org/10.1515/cls-2024-0003
[35] IS: 12269. Ordinary Portland cement 53 grade-specifications. Bureau of Indian Standards, 2013 New Delhi, India.
[36] IS: 383 Specification for coarse and fine aggregates from natural sources for concrete. Bureau of Indian Standards, 2016, New Delhi, India.
[37] IS: 456. Indian standard plain and reinforced concrete code of practice. Bureau of Indian Standards, 2016, New Delhi, India.
[38] IS: 9103. Concrete Admixtures Specification. Bureau of Indian Standards, 1999, New Delhi, India.
[39] IS: 1608-1. Metallic Materials Tensile Testing Part 1. Bureau of Indian Standards, 2018, New Delhi, India.
[40] Rama M, Shanthi VM. Study on Strength, Permeability and Micro-structure of Pervious Concrete Blended with Metakaolin. Jord J Civ Eng. 2023; 17 (1): https://doi.org/10.14525/JJCE.v17i1.02
[41] Stephen AA, Jeffrey M. Predictive Models for Evaluation of Compressive and Split Tensile Strengths of Recycled Aggregate Concrete Containing Lathe Waste Steel Fiber. Jord J Civ Eng, 2020; 14(4): 598-607.
[42] Jai KL, Sharma DK, Choudhary R, Bhargava S. Impact of Waste Iron Slag on Mechanical and Durability Properties of Concrete. Jord J of Civ Eng, 2023; 17 (1): 45-57. https://doi.org/10.14525/JJCE.v17i1.05
[43] Padmapriya R, Sudarsan JS, Nithiyanantham S. Formation of high strength concrete through sustainable waste materials as a partial replacement of cement. J Build Path Rehab. 2022; 7:86. https://doi.org/10.1007/s41024-022-00228-4
[44] IS: 10262. Concrete mix proportioning-Guidelines. Bureau of Indian Standards, 2009, New Delhi, India.
[45] IS: 516. Method of tests for strength of concrete. Bureau of Indian Standards, 2004 New Delhi, India.
[46] IS: 5816. Method of tests for strength of concrete. Bureau of Indian Standards, 2004, New Delhi, India.

[47] Masne N, Suryawanshi S. Evaluation of Ductility Ratio of Recycled Aggregate Concrete Beams Under Torsion. Recent Developments in Structural Engineering, 4: SEC 2023. Lecture Notes in Civil Engineering, 2024; 549:495-503. Springer, Singapore. https://doi.org/10.1007/978-981-97-6603-1_47
[48] Suryawanshi S, Singh B, Bhargava P. Equation for stress–strain relationship of recycled aggregate concrete in axial compression. Magaz Con Res. 2018; 163-171. https://doi.org/10.1680/jmacr.16.00108
[49] Earij A, Alfano G, Cashell K, Zhou X. Nonlinear three–dimensional finite–element modelling of reinforced– concrete beams: Computational challenges and experimental validation. Engin Fail Analy. 2017; 82: 92- 115. https://doi.org/https://doi.org/10.1016/j.engfailanal.2017.08.02